JOURNAL OF SPACECRAFT AND ROCKETS
Vol. 32, No. 2, March–April 1995

# New Gravity Compensation Method by Dither for Low-g Simulation

Saburo Matunaga*
*Tokyo Institute of Technology, Meguro, Tokyo 152, Japan*
and
Junjiro Onoda†
*The Institute of Space and Astronautical Science, Sagamihara, Kanagawa 229, Japan*

**As a new method for gravity compensation in two dimensions, it is proposed to decrease the time-average friction by use of in-plane vibration. This dither effect is investigated by using a mass that slides at a constant velocity on a level in-plane vibrating table. Its usefulness is further demonstrated by an experiment. An application of the method to gravity compensation is introduced. A motion test of a link structural model with ball-bearing supports and a level in-plane vibrating table is conducted to evaluate the performance. Experimental results show that the structure slides on the table with a drag-to-weight ratio of about $10^{-3}$ and drag-induced accelerations of about $10^{-3}g$.**

## Nomenclature

$A$ = amplitude of the table vibration
$\mathbf{f}$ = vector of Coulomb friction force
$f_d$ = amplitude of Coulomb friction force
$\bar{f}_{\parallel}$ = tangential time-average friction; see Eq. (9)
$\bar{f}_{\perp}$ = normal time-average friction; see Eq. (10)
$g$ = gravity acceleration, m/s$^2$
$I_i$ = inertia of the $i$th link, kg-m$^2$
$I_{\parallel}$ = tangential time-average friction ratio; see Eq. (11)
$I_{\perp}$ = normal time-average friction ratio; see Eq. (12)
$\mathbf{i}$ = unit vector corresponding to $x$ ($X$) direction
$\mathbf{j}$ = unit vector corresponding to $y$ ($Y$) direction
$K(k)$ = the first type of complete elliptic integral and its generic $k$
$\ell_i$ = length of the $i$th link, m
$m_i$ = mass of the $i$th link, kg
$\mathbf{r} \cdot \mathbf{v}$ = inner product between the vectors $\mathbf{r}$ and $\mathbf{v}$
$s_i$ = length ratio determining the position of the center of mass of the $i$th link
$\mathbf{U}$ = unit vector in the direction of the sliding velocity $\mathbf{V}$
$\mathbf{u}$ = unit vector in the direction of the relative sliding velocity $\mathbf{v}$
$V$ = sliding speed of the mass in the laboratory coordinate $O$-$XY$
$\mathbf{V}$ = sliding velocity of the mass in the laboratory coordinate $O$-$XY$
$\mathbf{v}$ = relative sliding velocity of the mass in the table-fixed coordinate $c$-$xy$
$\mathbf{W}$ = unit vector perpendicular to the sliding velocity $\mathbf{V}$
$X_c$ = $X$ component of the origin of the table-fixed coordinate $c$-$xy$ in the laboratory coordinate $O$-$XY$
$\mathbf{X}_c$ = direction vector of the table vibration
$\dot{\mathbf{X}}_c$ = velocity of the table vibration
$\theta$ = angle between the direction of the table vibration and the direction of the sliding velocity of the mass
$\kappa$ = dimensionless velocity parameter; see Eq. (8)
$\mu_d$ = coefficient of dynamic friction
$\mu_s$ = coefficient of static friction
$\tau$ = dimensionless time parameter; see Eq. (7)
$\omega$ = angular frequency of the table vibration

Presented as Paper 92-2275 at the AIAA/ASME/ASCE/AHS/ASC 33rd Structures, Structural Dynamics and Materials Conference, Dallas, TX, April 13–15, 1992; received May 11, 1993; revision received June 20, 1994; accepted for publication June 20, 1994. 

*Research Associate, Department of Mechano-Aerospace Engineering, 2-12-1 O-okayama, Meguro-ku, Tokyo 152, Japan. Member AIAA.

†Professor, Research Division of Space Transportation, 3-1-1 Yoshinodai. Member AIAA.

## Introduction

SIMULATING a microgravity environment in an on-ground laboratory is a difficult problem for experiments that attempt to evaluate dynamic behavior in space.[1] Usual gravity compensation methods for achieving the drag-free, zero-$g$ characteristics of space are classified as 1) inertial compensation, 2) neutral buoyancy, 3) floating, 4) sliding compensation, and 5) suspension. With inertial compensation, the simulated zero-$g$ condition is achieved by parabolic aircraft flights and by free-fall experiments in tall towers and in spacecraft. For neutral buoyancy, a very large water tank is used, and the spatial motion can be simulated. Floating methods use electromagnetic forces or air cushions, and sliding compensation methods use bladders, ice cubes, or bearings to reduce the friction force between test structures and a level table. In the suspension method, structures are suspended by wires. The level of the microgravity achieved by the above methods is on the order of $10^{-3}$–$10^{-5}g$ (inertial), $10^{-3}$–$10^{-4}g$ (floating), $10^{-2}$–$10^{-3}g$ (sliding), and $10^{-2}$–$10^{-4}g$ (suspension). The level achieved by neutral buoyancy is strongly dependent on the size, shape, and motion of the test structure.

When the sliding method is used, even the reduced friction may disturb the behavior of the test structure. The authors have studied the effectiveness of artificial dither for a further decrease of friction. For linearization purposes the dither is considered as a superimposed high-frequency signal.[2,3] An application of the dither to gravity compensation is proposed. Namely, a level in-plane vibrating table is used to reduce not the "real" friction but the time-average frictional force. The mechanism of this friction force reduction by vibration, or "dynamic lubrication,"[2] is discussed using a simple analytical model in order to clarify its physical meaning, and then demonstrated with an experiment. A behavior test of a link structural model with ball-bearing supports has also been conducted in order to evaluate the performance of this friction reduction method.

## Mechanism of Friction Reduction by Vibration

In order to investigate the mechanism of the proposed method, a simple analysis as shown in Fig. 1 is performed. A mass $m$ slides at a constant sliding velocity $\mathbf{V}$ on a level in-plane vibrating table, where $\mathbf{V}$ is measured with respect to the laboratory coordinates $O$-$XY$. The table is shaken sinusoidally with angular frequency $\omega$ and amplitude $A$ in the direction of $X$. Let $c$-$xy$ be defined as the table-fixed coordinates, and $X_c$ the $X$ component of the position of point

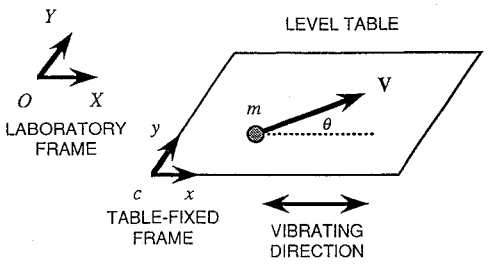


**Fig. 1 Analytical model.**

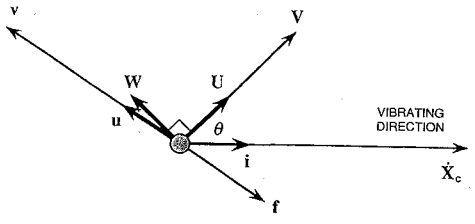


**Fig. 2 Definitions of vectors.**

$c$ with respect to $O$-$XY$. Then we can set $X_c = A \sin \omega t$, where $t$ is time. Further, the friction is assumed to follow the Coulomb model. The Coulomb friction **f** works on the mass in the opposite direction of the relative sliding velocity **v**:

$$\mathbf{v} = \mathbf{V} - \frac{\mathrm{d}X_c}{\mathrm{d}t}\mathbf{i}$$

$$= V\mathbf{U} - \omega A \cos \omega t \mathbf{i} \tag{1}$$

where **i**, **U** are the unit vectors along the $X$ axis and **V**, respectively, as shown in Fig. 2, and $V$ is the amplitude of **V**. Thus the Coulomb friction **f** can be expressed as follows:

$$\mathbf{f} = -\mu_d mg \frac{\mathbf{v}}{|\mathbf{v}|} = -f_d \mathbf{u} \tag{2}$$

$$f_d = \mu_d mg \tag{3}$$

where $\mu_d$ is the coefficient of dynamical friction, $g$ is the gravity acceleration, $f_d$ is the amplitude of the friction, and **u** is the unit vector along **v**, given by

$$\mathbf{u} = p\mathbf{U} - q\mathbf{i} \tag{4}$$

$$p = \frac{\kappa}{\sqrt{\kappa^2 - 2\kappa \cos\theta \cos\tau + \cos^2\tau}} \tag{5}$$

$$q = \frac{\cos\tau}{\sqrt{\kappa^2 - 2\kappa \cos\theta \cos\tau + \cos^2\tau}} \tag{6}$$

where $\theta$ is the angle of **V** with the $X$ axis and we define the dimensionless time

$$\tau = \omega t \tag{7}$$

and the velocity parameter

$$\kappa = \frac{V}{\omega A} \tag{8}$$

Figure 3 illustrates the mechanism of friction reduction by means of vibration. The relative velocity **v** rapidly changes direction in accordance with the vibration of the table, and the direction of the Coulomb friction force **f** also changes. While the amplitude of **v** changes, the amplitude of **f** remains constant. Consequently, the frictional force in the direction of **V** decreases on time average.

In order to perform a quantitative investigation of this fact, the effective (time-average) frictional forces are defined as follows:

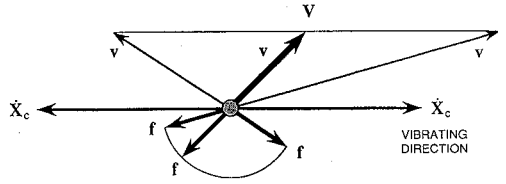


**Fig. 3 Mechanism of time-average friction reduction.**

tangential

$$\bar{f}_{\parallel} = -\lim_{T\to\infty} \frac{1}{\omega T} \int_0^{\omega T} \mathbf{f} \cdot \mathbf{U}\, \mathrm{d}\tau \tag{9}$$

and normal

$$\bar{f}_{\perp} = -\lim_{T\to\infty} \frac{1}{\omega T} \int_0^{\omega T} \mathbf{f} \cdot \mathbf{W}\, \mathrm{d}\tau \tag{10}$$

where **W** is the unit vector perpendicular to **V** as shown in Fig. 2. From these expressions, the directional time-average friction ratios are defined as follows:
tangential

$$I_{\parallel}(\kappa, \theta) = \frac{\bar{f}_{\parallel}}{f_d} \tag{11}$$

and normal

$$I_{\perp}(\kappa, \theta) = \frac{\bar{f}_{\perp}}{f_d} \tag{12}$$

After some calculation using the periodicity in this analysis, we obtain

$$\frac{\bar{f}_{\parallel}}{f_d} = \frac{1}{2\pi} \int_0^{2\pi} \frac{\kappa - \cos\theta \cos\tau}{\sqrt{\kappa^2 - 2\kappa \cos\theta \cos\tau + \cos^2\tau}}\, \mathrm{d}\tau \tag{13}$$

$$\frac{\bar{f}_{\perp}}{f_d} = \frac{1}{2\pi} \int_0^{2\pi} \frac{\sin\theta \cos\tau}{\sqrt{\kappa^2 - 2\kappa \cos\theta \cos\tau + \cos^2\tau}}\, \mathrm{d}\tau \tag{14}$$

The above integrals can be calculated explicitly if $\theta = 0$ and 90 deg, respectively, as follows:

$$I_{\parallel}(\kappa, 0\ \mathrm{deg}) = \begin{cases} \dfrac{2}{\pi} \sin^{-1}\kappa & (0 \le \kappa \le 1) \\ 1 & (\kappa > 1) \end{cases} \tag{15}$$

$$I_{\parallel}(\kappa, 90\ \mathrm{deg}) = \frac{2}{\pi} \frac{\kappa}{\sqrt{\kappa^2 + 1}} K(k) \tag{16}$$

$$I_{\perp}(\kappa, 0\ \mathrm{deg}) = I_{\perp}(\kappa, 90\ \mathrm{deg}) = 0 \tag{17}$$

where $k = \sqrt{1/(\kappa^2 + 1)}$ and $K(k)$ is the first type of complete elliptic integral. Figure 4 shows the values of $I_{\parallel}$ and $I_{\perp}$, where the horizontal axes represent values of the velocity parameter $\kappa$. Note that the ratio of the time-average friction to the dynamic friction decreases as the velocity parameter $\kappa = V/\omega A$ decreases. Note also that $I_{\parallel}(\kappa, \theta) < 1$ if $\theta \neq 0$ in the case of $\kappa \ge 1$ although $I_{\parallel}(\kappa, \theta) = 1$ if $\theta = 0$, because the friction force perpendicular to the constant sliding velocity **V** does no work. We can prove analytically the convergence of $I_{\perp}(\kappa, \theta)$ to zero in the neighborhood of $\kappa = 1$ if $\theta \to 0$.

It is important to emphasize that Eq. (15) is essentially equivalent to the dual-input describing function of odd saturating nonlinearities if sinusoidal dither is added. In linearizing the nonlinearity of small input signals triangular dither is preferable to sinusoidal dither in that it provides a larger linear region.[3] On the other hand, square-wave dither is best for friction reduction, because in theory the friction completely vanishes in the range $0 \le \kappa \le 1$. Practically, though, sinusoidal dither may be the best waveform for the friction

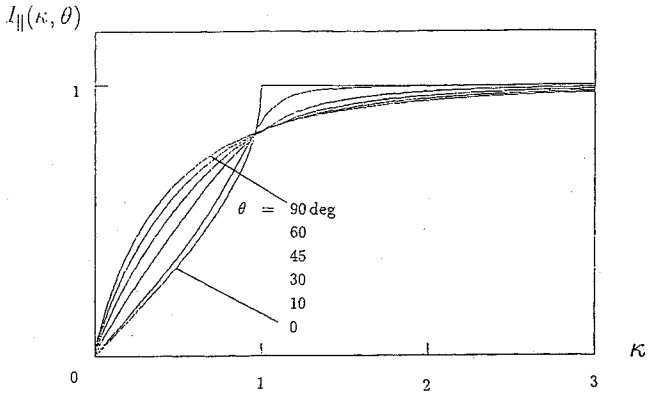


a) Tangential

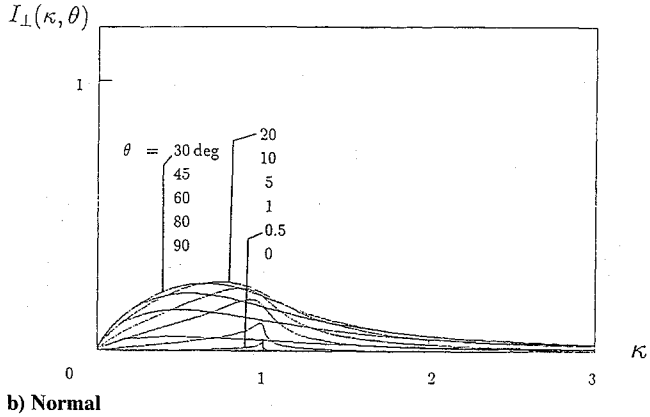


b) Normal

Fig. 4 Time-average friction ratio—theory.

reduction method. More quantitative analyses, including dynamic effects, will be needed for evaluating the dither waveform and other parameters.

## Demonstration of Experiment

In this section, an experiment is conducted to verify the result of the above analysis. The schematic diagram of the experiment is shown in Fig. 5.

A brass right-cylinder-form weight (2116 g) is put on a level table (1200 × 1200 mm), which is vibrated by a shaker. The frequency and amplitude of the table vibration are measured by an optical displacement gauge and a FFT analyzer. The weight is pulled by an autograph through a pulley at a constant velocity, and the dynamic frictional force applied to the weight is measured by a load cell equipped with an autograph. The tangential time-average friction can be obtained only approximately in this experiment, because the weight moves in a rocking fashion and does not always slide at a constant velocity. Two cases of the sliding direction, $\theta = 0$ and 90 deg, were chosen. The pulling speed of the weight was chosen in the range of 1–10 mm/s. The frequency range of the table vibration is from 10 to 70 Hz, and the amplitude of the vibration is chosen in the range of 0.02–0.5 mm.

Some results are shown in Fig. 6, where the horizontal and vertical axes represent values of the dimensionless velocity parameter and the tangential time-average friction, respectively. The black circles represent the average values of tangential time-average friction for each velocity parameter $\kappa$. The triangles and rhombuses correspond, respectively, to the upper and bottom values. The solid lines are theoretical curves. Figure 6 indicates that the friction ratios obtained in the experiment have the same form as that obtained from previous analysis, but they have higher values. The most important reason for this result is thought to be the omission of dynamic effects in the theoretical analysis of the previous section. The essence of the proposed friction reduction method is to change the direction of the friction smoothly around the direction of motion of the mass, using the table vibration. When rocking or stick-slip motion occurs,

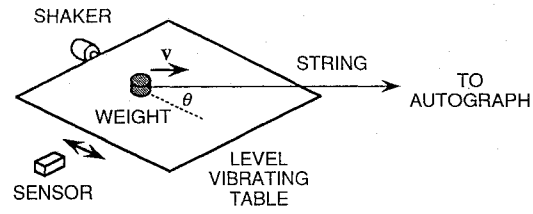


Fig. 5 Schematic view of the experimental setup.

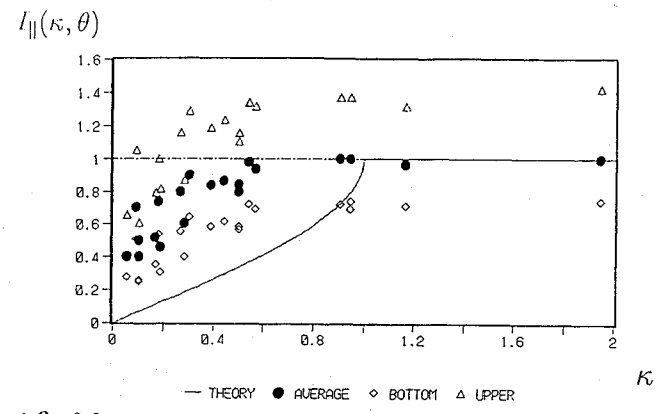


a) $\theta = 0$ deg

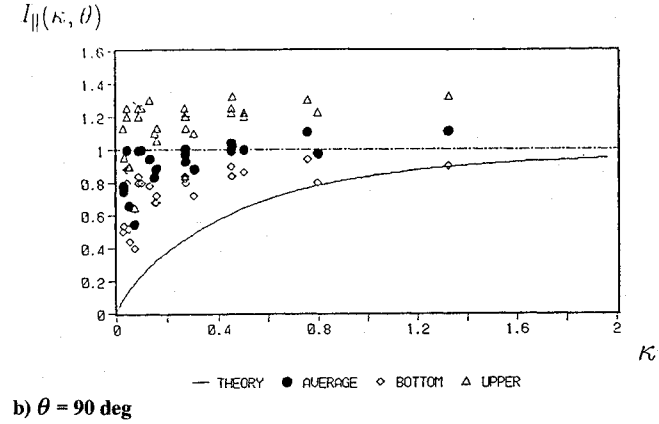


b) $\theta = 90$ deg

Fig. 6 Time-average friction ratio—experiment.

the direction of the friction does not change smoothly. Thus, the reduction of the average frictional force does not work well. In this experiment, however, the dynamic friction can be reduced by a factor of 0.4 (60%) through vibration.

## Behavior Test of a Link Structure

### Ball-Bearing Support

The application of friction reduction by vibration to gravity compensation can be expected to be successful. In particular, the use of sliding compensation with this method is preferable because of its low cost. The authors assembled a ball-bearing support[4] as shown in Fig. 7 in order to demonstrate sliding compensation using friction reduction by vibration. The support is composed of a ball-bearing part and a spring-oil-damper part. The ball bearing consists of a large main ball surrounded by hundreds of smaller balls, and its starting friction coefficient is 0.013. The main purpose of the spring in the spring-oil-damper part is to correct for the deviation of height due to the geometrical change of the structure which can deform. The purpose of the damper is to suppress the vertical vibration caused by the table vibration. The principle characteristics of the ball-bearing support are 1) somewhat lower friction, 2) low cost of production and maintenance, 3) small and light weight (about 70 g), 4) easy operation, and 5) no restriction of operation time.

**Table 1 Specifications of the link structural model**

| Link $i$ | Length, m $l_i$ | $s_i$ | Mass $m_i$, kg | Moment of inertia $I_i$, kg-m$^2$ |
|---|---|---|---|---|
| 1 | 0.300 | 0.410 | 1.235 | 0.0272 |
| 2 | 0.300 | 0.500 | 1.011 | 0.0232 |
| 3 | 0.300 | 0.500 | 1.168 | 0.0255 |
| 4 | 0.300 | 0.427 | 1.182 | 0.0263 |

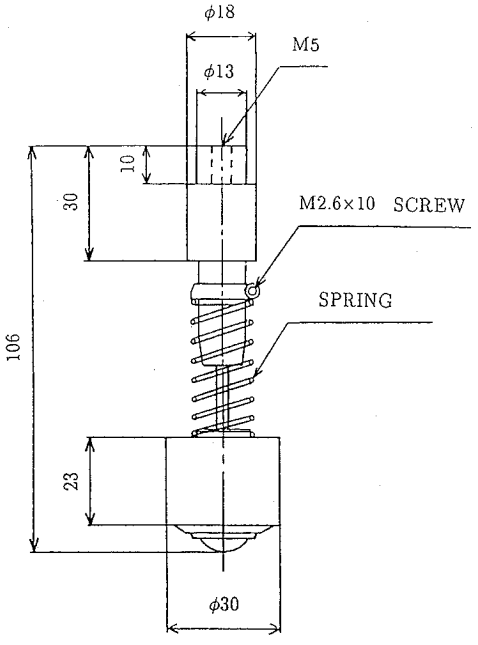


**Fig. 7 Ball-bearing support.**

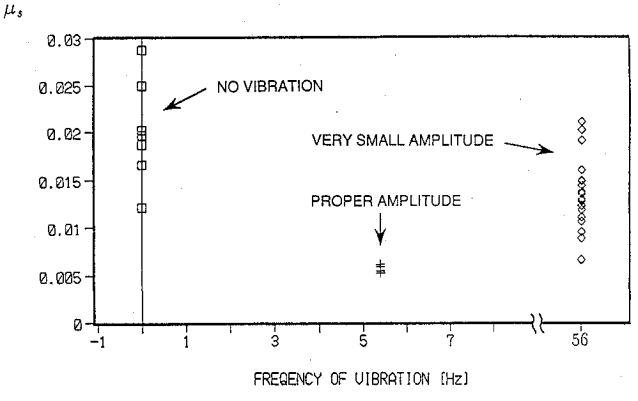


**Fig. 8 Coefficient of the static friction of ball-bearing supports.**

Figure 8 shows the coefficient of static friction of the ball-bearing support with the addition of vibration, where the horizontal axis represents the frequency of vibration. We can see that the ball bearing is able to move smoothly and stably, and that its coefficient of static friction can be decreased to $0.006 \approx 10^{-3}$ by means of proper vibration.

### Motion Test of a Link Structure

A two-dimensional motion test of a link structural model using sliding compensation with friction reduction by vibration has been conducted in order to simulate the behavior of the structure in space. The objective of this experiment is to evaluate the microgravity level achieved by this compensation method through comparison between experimental results and theoretical calculations. Figure 9 shows the outline of the link structural model used in this experiment. Specifications are listed in Table 1. The link structure has three degrees of freedom in rotation with five ball-bearing supports, and

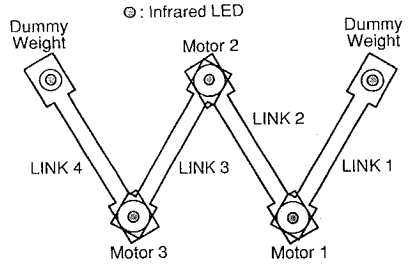


**Fig. 9 Link structural model.**

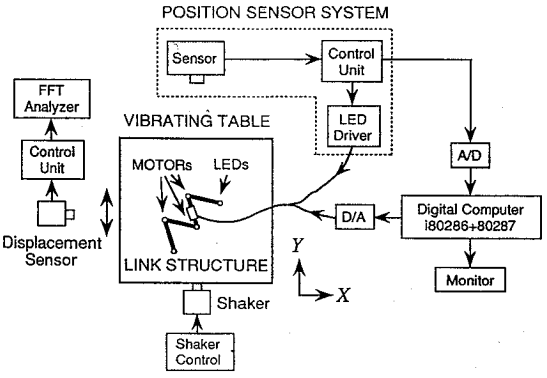


**Fig. 10 Block diagram of the experimental setup.**

is thought to be one of the simplest variable-geometry structures to be able to execute an arbitrary motion in space, because it has no large massive part as a space robot manipulator does.

Figure 10 shows a block diagram of the experimental system. It is composed of an in-plane vibrating table (1200 × 1200 mm), a position sensor consisting of infrared LEDs and a camera, and a personal computer ($i$80286 + 80287) to drive the analog-to-digital and digital-to-analog converters. The frequency and amplitude of the vibrating table are measured by an optical displacement gauge and a FFT analyzer. The errors of sensed positions due to the orientation of the camera and the parameters are corrected by an iterative least-squares method. The positions are sensed by the camera suspended at a height of 3 m, and the position accuracy is 9 mm.

The authors conducted a simple motion test of the link structure driven by one stepper motor between link 1 and 2. Figure 11 shows the experimental results: Fig. 11a presents a trace of the sensed motion of the structure every second (the numbers represent distance in meters), Fig. 11b presents the corresponding theoretical calculation, Fig. 11c expresses the deviation (in meters) of the position of the center of gravity, and Fig. 11d shows the attitude (in degrees) of link 1. The horizontal axes in both Figs. 11c and 11d represent time in seconds. Figure 11b was calculated under the principle of momentum conservation for the case of no external disturbances. As shown in Fig. 11d, in the case of a vibrating table, the maximum error of the attitude is about 5 deg ≈ 0.09 rad, and in the case of no vibration, the maximum is about 15 deg ≈ 0.26 rad. Thus the effectiveness of the vibration-induced friction reduction is validated by the experiment.

Figure 12 shows the acceleration of the center of gravity of the link structure, $\alpha$ calculated from the sensed positions during the motion in Fig. 11. We see that the structure slides on the table with drag-induced accelerations less than $10^{-3}g$ on average. When, however, more complex motion of the structure is performed, as shown for example in Fig. 13, simulating a docking construction[4] of two moving structures (where the moving target represents the end effector of another structure), then the sensed acceleration at the center of gravity is on the order of $10^{-3}g$ as shown in Fig. 14. It is concluded that this is a reasonable result, considering the coefficient of friction of the ball-bearing support as given in Fig. 8. Both the drag-to-weight ratio and drag-induced accelerations achieved in this gravity compensation system are on the order of about $10^{-3}$ on average, and the performance is excellent in spite of the very low development cost of the system.

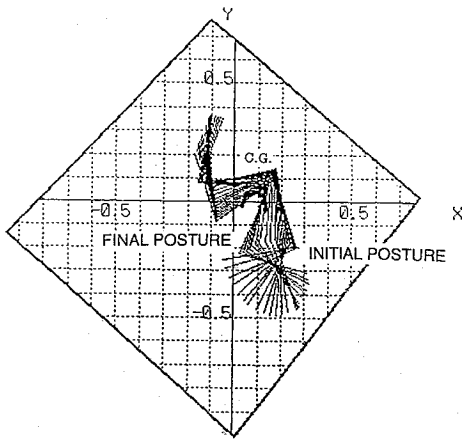


a) Experiment

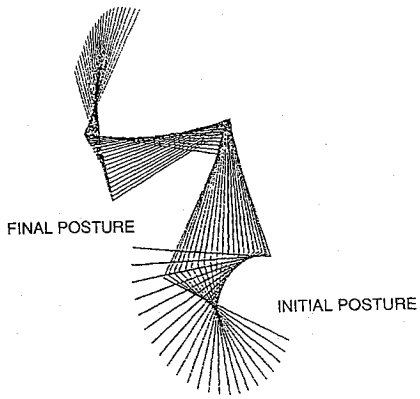


b) Calculation

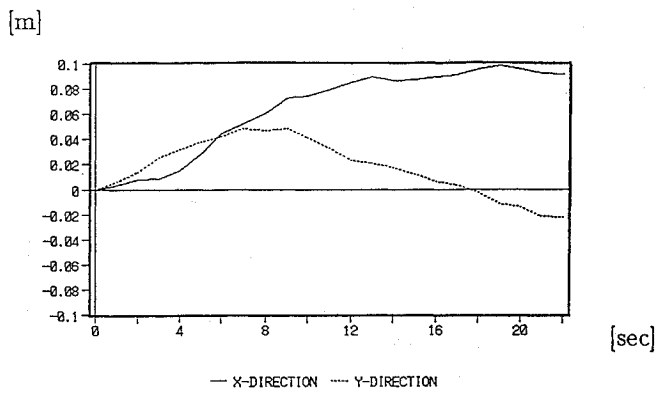


c) Position of center of gravity

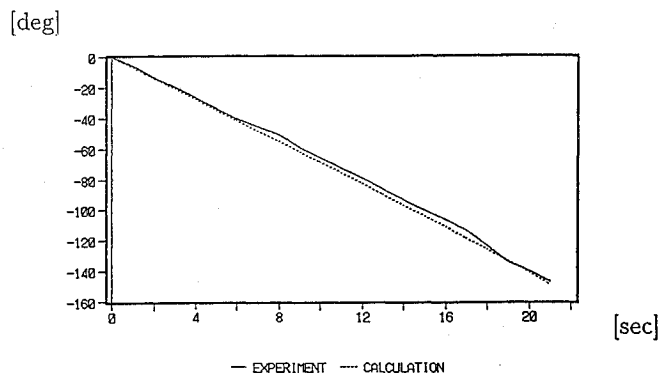


d) Attitude of link 1

Fig. 11 Experimental results—case 1.

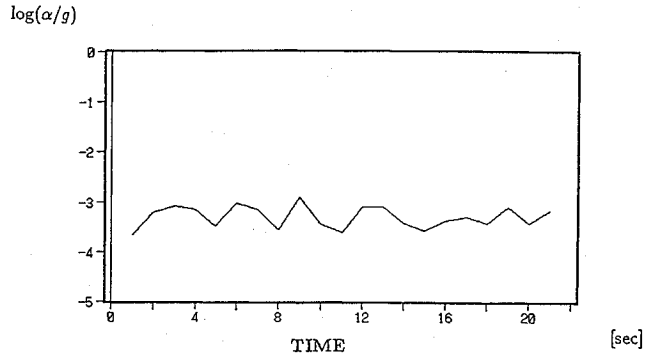


Fig. 12 Property of gravity compensation—case 1.

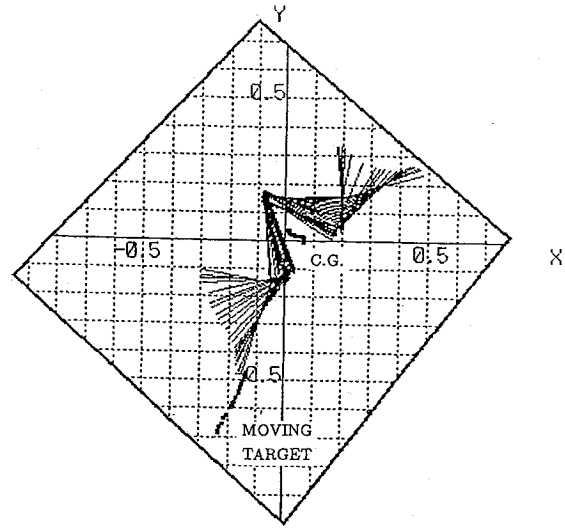


a) Experiment

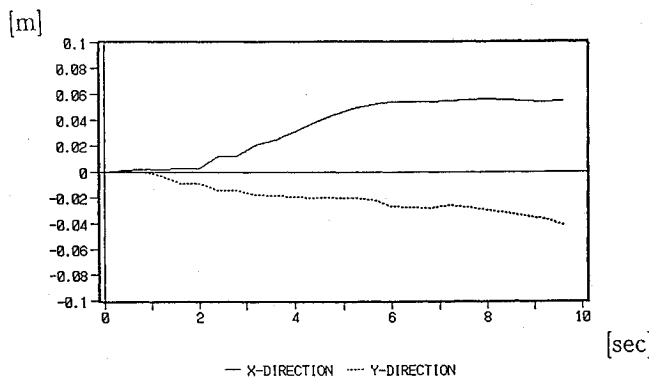


b) Position of center of gravity

Fig. 13 Experimental results—case 2 (capture of target).

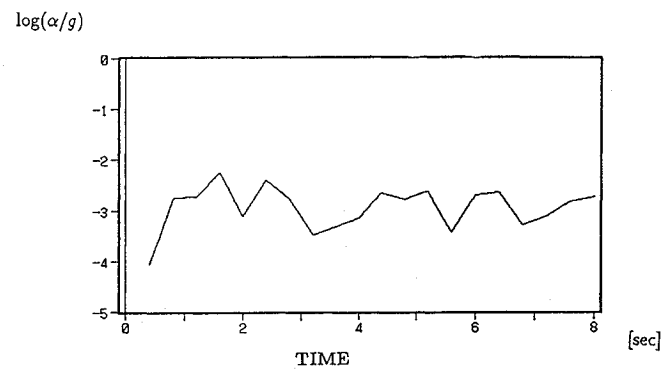


Fig. 14 Property of gravity compensation—case 2.

## Concluding Remarks

A new gravity compensation system for the two-dimensional motion test is proposed. This is an application of the fact that the effective Coulomb friction is diminished by using a vibrating table on account of the dither effect. The mechanism of friction reduction by vibration was investigated by using an analytical model and an experiment to clarify its physical meaning. These investigations show that the ratio of time-average friction to the dynamical friction decreases as the velocity parameter $V/\omega A$ decreases. The authors developed a sliding gravity compensation system using a level vibrating table. A ground behavior test of a link structural model equipped with ball-bearing supports was conducted in order to evaluate the performance of this system. Experimental results showed that this structure slides on the table with a drag-to-weight ratio of about $10^{-3}$ and drag-induced accelerations of about $10^{-3}g$. Note that this method can also be applied to some types of large-space-structure experiments, such as vibration tests of long beam-like structures, if small vibrating tables are appropriately used.

Further studies on friction reduction by vibration are needed, including flexibility, dynamic effects, applications to actual tests, and extension to multidirectional vibration.

## Acknowledgments

The authors greatly thank K. Ichida (Institute of Space and Astronautical Science), Y. Miyazaki (University of Tokyo) and T. Kayashima (Nihon University) for their assistance with the experiments.

## References

[1]Hanks, B. R., and Pinson, L. D., "Large Space Structures Raise Testing Challenges," *Astronautics and Aeronautics*, Oct. 1983, pp. 34–40, 53.

[2]Elgerd, O. I., *Control Systems Theory*, McGraw-Hill, New York, 1967, p. 322.

[3]Gelb, A. G., and Vander Verde, W. E., *Multiple-Input Describing Functions and Nonlinear System Design*, McGraw-Hill, New York, 1968, pp. 345–359.

[4]Matunaga, S., Miura, K., and Natori, M., "A Construction Concept of Large Space Structures Using Intelligent/Adaptive Structures," *Proceedings of AIAA/ASME/ASCE/AHS/ASC 31st Structures, Structural Dynamics and Materials Conference* (Long Beach, CA) AIAA, Washington, DC, 1990, pp. 2298–2305 (AIAA Paper 90-1128).

E. A. Thornton
*Associate Editor*